HHS Public Access

Author manuscript

Science. Author manuscript; available in PMC 2017 May 25.

Published in final edited form as:

Science. 2016 August 05; 353(6299): 603–608. doi:10.1126/science.aaf6803.

RIPK1 Mediates Axonal Degeneration By Promoting Inflammation and Necroptosis in ALS

Yasushi Ito[1], **Dimitry Ofengeim**[1], **Ayaz Najafov**[1], **Sudeshna Das**[2], **Shahram Saberi**[3], **Ying Li**[1,4], **Junichi Hitomi**[1], **Hong Zhu**[1], **Hongbo Chen**[1], **Lior Mayo**[6], **Jiefei Geng**[1], **Palak Amin**[1], **Judy Park DeWitt**[1], **Adnan Kasim Mookhtiar**[1], **Marcus Florez**[1], **Amanda Tomie Ouchida**[1], **Jian-bing Fan**[5], **Manolis Pasparakis**[7], **Michelle A. Kelliher**[8], **John Ravits**[3], and **Junying Yuan**[1,*]

[1]Department of Cell Biology, Harvard Medical School, 240 Longwood Ave. Boston, MA 02115, USA

[2]MassGeneral Institute for Neurodegenerative Disease, Massachusetts General Hospital, Cambridge, MA 02139; Department of Neurology, Harvard Medical School, Boston, MA 02115, USA

[3]ALS Translational Research Program, Department of Neurosciences, University of California, San Diego, USA

[4]Interdisciplinary Research Center on Biology and Chemistry, Shanghai Institute of Organic Chemistry, Chinese Academy of Sciences, 26 QiuYue Rd, PuDong District, Shanghai, 201203, China

[5]Illumina, Inc. San Diego, CA 92122, USA

[6]Ann Romney Center for Neurologic Diseases, Brigham and Women's Hospital, Harvard Medical School, Boston, MA, USA

[7]Institute for Genetics, University of Cologne, 50674 Cologne, Germany

[8]Department of Cancer Biology, University of Massachusetts Medical School, Worcester, MA 01605, USA

Abstract

Mutations in Optineurin (*Optn*) gene have been implicated in both familial and sporadic amyotrophic lateral sclerosis (ALS). However, the role of this protein in the central nervous system (CNS) and how it may contribute to ALS pathology is unclear. Here, we found that optineurin actively suppressed RIPK1-dependent signaling by regulating its turnover. Loss-of-OPTN led to progressive dysmyelination and axonal degeneration through engagement of necroptotic machinery, including RIPK1, RIPK3 and MLKL, in the CNS. Furthermore, RIPK1/RIPK3-mediated axonal pathology was commonly observed in $SOD1^{G93A}$ transgenic mice and

*Correspondence to: Junying Yuan. jyuan@hms.harvard.edu.

Supplementary Materials

Materials and Methods

Figs. S1–S8.

Tables. S1–S4.

pathological samples from human ALS. Thus, RIPK1/RIPK3 plays a critical role in mediating progressive axonal degeneration and inhibiting RIPK1 kinase may provide an axonal protective strategy for the treatment of ALS and other human degenerative diseases characterized by axonal degeneration.

Loss-of-function mutations in the Optineurin (*Optn*) gene have been implicated in both familial and sporadic cases of amyotrophic lateral sclerosis (ALS), a devastating degenerative motor neuron disease (1–3). The *Optn* gene encodes a ubiquitin-binding protein involved in TNFα signaling but is dispensable for NF-κB activation (4, 5). It is still unclear how the loss of function of *Optn* leads to human ALS.

RIPK1 is a critical regulator of cell death and inflammation (6). RIPK1 regulates necroptosis, a form of regulated necrotic cell death, by promoting the sequential activation of two downstream targets, RIPK3 and MLKL (7–9). Application of Nec-1s, a highly specific inhibitor of RIPK1 kinase activity, blocks necroptosis and inflammation in vitro and in vivo (10, 11). However, the pathophysiological significance of RIPK1 and necroptosis in the genetic context of human diseases remains to be established.

Axonal degeneration is frequently observed before the death of neuronal cell bodies in patients with neurodegenerative disorders including ALS and contributes significantly to neurological disability (12). Axonal degeneration induced by direct nerve injury, known as Wallerian degeneration, is mediated through a mechanism distinct from apoptosis of neuronal cell bodies (13, 14). Axonal degeneration in patients with neurodegenerative diseases may also exhibit features similar to Wallerian degeneration and is referred to as “Wallerian-like” degeneration. The mechanism of Wallerian degeneration is still unclear.

To understand the mechanism by which the loss of OPTN could lead to ALS, we developed *Optn*−/− mice (fig. S1A–B). We examined the impact of *Optn* loss in the spinal cord of *Optn* −/− mice. We found that the number and morphology of spinal cord motor neurons in *Optn* −/− mice were indistinguishable from WT mice (fig. S1C–D). However, we observed a marked reduction in the number of motor axons and abnormal myelination in the ventrolateral spinal cord white matter in the *Optn*−/− mice from 3 weeks to 2 years (Fig. 1A–D; fig. S1E). The axonal pathology presented as a decompaction of myelin sheaths with a decreased g-ratio, an increased large-diameter axons and a decreased axonal number in the ventrolateral white matter (Fig. 1B–D), suggesting degeneration and swelling of motor neuron axons in *Optn*−/− mice. This finding is similar to axonal pathology observed in the spinal cords of ALS patients in early stages of the disease (15). The pathology was progressive as a reduction in axonal numbers was observed at 12 weeks or older but not at 3 weeks (fig. S1F). Similar pathology was observed in the ventral roots of motor axons in *Optn*−/− mice (fig. S1G–J). In addition, denervation of neuromuscular junctions in the tibialis anterior muscle was observed in *Optn*−/− mice (fig. S1K–L). Thus, OPTN deficiency leads to axonal pathology without affecting motor neuron cell bodies. Consistent with this notion, we observed a significant increase in the number of TUNEL+ in the ventrolateral white matter of spinal cords of *Optn*−/− mice (Fig. 1E). Thus, OPTN deficiency sensitizes cells to non-apoptotic cell death in *Optn*−/− mice.

To determine the cell types involved in mediating OPTN-deficiency-induced axonal degeneration, we generated lineage-specific deletion of OPTN using *Cnp-cre*, *Lyz2-cre, Gfap-cre* and *Mnx1-cre* mice (16–18) (fig. S2). Loss of OPTN from oligodendrocytes and myeloid cells, but not that of astrocytes or motorneurons were sufficient to reproduce axonal myelination pathology (Fig. 1F–I). Furthermore, we induced OPTN loss from microglial lineage by dosing $Optn^{F/F}; Cx3cr1^{Cre}$ mice (19) with tamoxifen for one month (fig S3A) and also found axonal pathology as that in *Optn*−/− mice (fig. S3B–E).

Because necroptosis is an important non-apoptotic cell death *mechanism* (20), we searched our dataset for genes that could sensitize to necroptosis (21). Knockdown of *Optn* sensitized L929 cells to necroptosis induced by TNFα or zVAD.fmk, the latter is known to involve TNFα autocrine (Z-score = −2.07, Table S1; fig. S4A–B) (22). Thus, *Optn* deficiency sensitized to necroptosis (fig. S4C). The biochemical hallmarks of necroptosis, including the upshifts of RIPK1, RIPK3 and p-MLKL, and the levels of complex IIb were significantly higher in *Optn*−/− MEFs than in *Optn*+/+ MEFs (fig. S4D). Importantly, *Optn*−/− oligodendrocytes were sensitized to die by TNFα-induced necroptosis which was protected by Nec-1s and in *Optn*−/−; $Ripk1^{D138N/D138N}$ and *Optn*−/−; *Ripk3*−/− double mutants (23, 24) (Fig. 2A). Thus, we conclude that OPTN deficiency can promote necroptosis of oligodendrocytes.

The expression levels of RIPK1, RIPK3 and MLKL, the key mediators of necroptosis, were all increased in the spinal cords of *Optn*−/− mice (Fig. 2B). Furthermore, we detected the interaction of OPTN and RIPK1 in WT spinal cords (Fig. 2C). Compared to WT mice, RIPK1 K48 ubiquitination levels were decreased while RIPK1 mRNA unchanged in the spinal cords of *Optn*−/− mice (Fig. 2D–E). Furthermore, RIPK1 was degraded slower in *Optn*−/− MEFs than that in WT cells (Fig. 2F). Thus, OPTN might control sensitivity to necroptosis by regulating proteasomal turnover of RIPK1.

Phosphor-Ser14/15, a marker of RIPK1 activation, was increased in *Optn*−/− microglia relative to WT microglia, which was inhibited by Nec-1s and $Ripk1^{D138N/D138N}$ mutation (Fig. 2G). Because microglia express little MLKL, we hypothesize that RIPK1 activation in microglia promotes inflammatory signaling, not necroptosis. Consistently, we detected an increased production of multiple proinflammatory cytokines, including IL1α, IL1β, IL2, IL12, IFNγ and TNFα in the spinal cords of *Optn*−/− mice, which were markedly reduced in the *Optn*−/−; $Ripk1^{D138N/D138N}$ mice (Fig. 2H). In addition, *Optn*−/− microglia had elevated TNFα, which was inhibited by Nec-1s (fig. S5A). Consistently, the levels of TNFα were also increased in the spinal cords of $Optn^{F/F}; Lyz2\text{-}cre$ mice (fig. S5B).

To explore the effect of OPTN deficiency on transcriptions, we performed RNA-seq on WT, *Optn*−/−, and *Optn*−/−; $Ripk1^{D138N/D138N}$ primary microglia. Co-expression analysis (25) identified a module with approximately 1300 genes (ME1) differentially-expressed between WT and *Optn*−/− microglia and suppressed by $Ripk1^{D138N/D138N}$. The top 71 genes in this module include the LPS receptor CD14 and CD86, a biomarker for the proinflammatory M1-like state (26) (Fig. 2I; Table S2). Elevated CD14 and CD86 in *Optn*−/− microglia were suppressed by Nec-1s and $Ripk1^{D138N/D138N}$ (fig. S5C). Thus, OPTN deficiency promotes an M1-like inflammatory microglia.

We analyzed the genes differentially expressed in *Optn*−/− microglia using MSigDB (Molecular Signatures Database) (27) to identify transcription factors whose targets were overrepresented. We found a significant overrepresentation of the predicted Sp1 transcription factor targets in ME1 module (Table S3) with a network (28) of 225 Sp1 targets regulated by RIPK1 (fig. S6A). We found that increased production of TNFα and death of L929 cells can be blocked by knockdown of Sp1 and by Nec-1s (fig. S6B–C). Thus, loss-of-OPTN in the spinal cord may increase RIPK1-dependent inflammation.

We examined the involvement of necroptosis in *Optn*−/− mice in vivo. We found that the increase in TUNEL+ cells and axonal pathology of *Optn*−/− mice were all rescued in the *Optn*−/−; *Ripk1*$^{D138N/D138N}$ double mutant and the *Optn*−/−; *Ripk3*−/− double mutant mice, and by Nec-1s (Fig. 3A–E). Behaviorally, *Optn*−/− mice showed no difference in the total locomotor activity while the vertical rearing activity was significantly reduced compared to that of WT mice (Fig. 3F–H). These data suggest that OPTN deficiency leads to hindlimb weakness. Furthermore, the vertical rearing deficit in *Optn*−/− mice was rescued pharmacologically by Nec-1s and genetically in the *Optn*−/−; *Ripk1*$^{D138N/D138N}$ mice and *Optn*−/−; *Ripk3*−/− mice. Thus, OPTN deficiency leads to the activation of necroptotic machinery to promote axonal pathology.

To explore the involvement of RIPK1 mediated axonal pathology in ALS in general, we used *SOD1*^{G93A} transgenic mice. Early degeneration of oligodendrocytes *SOD1*^{G93A} mice was reported but mechanism is unclear (29). We found that the expression of RIPK1, RIPK3 and MLKL in the spinal cords of *SOD1*^{G93A} transgenic mice was elevated (Fig. 4A). In addition, we observed a similar axonal pathology as that of *Optn*−/− mice in *SOD1*^{G93A} mice before the onset of motor dysfunction (Fig. 4B–C). Furthermore, these axonal myelination defects were blocked and motor dysfunction onset delayed by genetically *Ripk3* knockout or by oral administration of Nec-1s (Fig. 4D–E). Thus, while we cannot rule out the contribution of RIPK1 or other pro-apoptotic factors to the degeneration of motor neuron cell bodies (30, 31), the activation of necroptosis contributes to axonal pathology and motor dysfunction in the *SOD1*^{G93A} transgenic mice.

We next characterized the role of RIPK1 and necroptosis in human ALS. We found evidence of demyelination in the lateral column white matter of lower spinal cord pathological samples from ALS patients as reported (Fig. 4F). In human ALS pathological samples, we also detected multiple biochemical hallmarks of necroptosis including increased levels of RIPK1, RIPK3 and MLKL and increased RIPK1 p-Ser14/15 and p-MLKL in both microglia and oligodendrocytes (Fig. 4G; fig. S7; Table S4). Importantly, p-MLKL was primarily localized in the white matter, where demyelination was found.

Taken together, our results provide a direct connection between Wallerian-like degeneration induced by OPTN deficiency and RIPK1 regulated necroptosis and inflammation. By promoting both inflammation and cell death, RIPK1 may be a common mediator of axonal pathology in ALS (fig. S8). Because RIPK1 is recruited specifically to TNFR1 to mediate the deleterious effect of TNFα (32), blocking RIPK1 may provide a therapeutic option for the treatment of ALS without affecting TNFR2. Finally, given the recruitment of OPTN to intracellular protein aggregates found in pathological samples from patients with

Alzheimer's disease, Parkinson's disease, Creutzfeldt-Jakob disease, multiple system atrophy and Pick's disease (33, 34), a possible role of RIPK1 in mediating the wide presence of axonal degeneration in different neurodegenerative diseases should be considered.

Supplementary Material

Refer to Web version on PubMed Central for supplementary material.

Acknowledgments

This work was supported in part by grants from the NINDS-US (1R01NS082257), the NIA - US (1R01AG047231) and by the National Science and Technology Major Project of China (No. 2014ZX09102001-002) (to JY) and NIAID (2RO1AI075118) (to MK). YI was supported in part by postdoctoral fellowships from Japan (Daiichi Sankyo Foundation of Life Science, The Nakatomi Foundation, the Mochida Memorial Foundation for Medical & Pharmaceutical Research, and Japan Society for the Promotion of Science). DO was supported by a postdoctoral fellowship from the National Multiple Sclerosis Society and a National MS Society Career Transition Award. HC was supported by a grant from Huazhong University of Science and Technology, Wuhan, China. We thank Dr. B. Caldarone of NeuroBehavior Laboratory, Harvard Institute of Medicine, for conducting mouse behavior analysis, Dr. J. Walters at the HMS Nikon microscope facility for fluorescence microscopy and Dr. M. Ericsson of the Electron Microscopy Facility at Harvard Medical School for EM analysis.

References and notes

1. Beeldman E, et al. A Dutch family with autosomal recessively inherited lower motor neuron predominant motor neuron disease due to optineurin mutations. Amyotroph Lateral Scler Frontotemporal Degener. 2015; 16:410–411. [PubMed: 26203661]
2. Cirulli ET, et al. Exome sequencing in amyotrophic lateral sclerosis identifies risk genes and pathways. Science. 2015; 347:1436–1441. [PubMed: 25700176]
3. Maruyama H, et al. Mutations of optineurin in amyotrophic lateral sclerosis. Nature. 2010; 465:223–226. [PubMed: 20428114]
4. Munitic I, et al. Optineurin insufficiency impairs IRF3 but not NF-kappaB activation in immune cells. J Immunol. 2013; 191:6231–6240. [PubMed: 24244017]
5. Zhu G, et al. Optineurin negatively regulates TNFalpha- induced NF-kappaB activation by competing with NEMO for ubiquitinated RIP. Curr Biol. 2007; 17:1438–1443. [PubMed: 17702576]
6. Ofengeim D, Yuan J. Regulation of RIP1 kinase signalling at the crossroads of inflammation and cell death. Nat Rev Mol Cell Biol. 2013; 14:727–736. [PubMed: 24129419]
7. He S, et al. Receptor interacting protein kinase-3 determines cellular necrotic response to TNF-alpha. Cell. 2009; 137:1100–1111. [PubMed: 19524512]
8. Sun L, et al. Mixed lineage kinase domain-like protein mediates necrosis signaling downstream of RIP3 kinase. Cell. 2012; 148:213–227. [PubMed: 22265413]
9. Zhang DW, et al. RIP3, an energy metabolism regulator that switches TNF-induced cell death from apoptosis to necrosis. Science. 2009; 325:332–336. [PubMed: 19498109]
10. Degterev A, et al. Identification of RIP1 kinase as a specific cellular target of necrostatins. Nat Chem Biol. 2008; 4:313–321. [PubMed: 18408713]
11. Degterev A, et al. Chemical inhibitor of nonapoptotic cell death with therapeutic potential for ischemic brain injury. Nat Chem Biol. 2005; 1:112–119. [PubMed: 16408008]
12. Conforti L, Gilley J, Coleman MP. Wallerian degeneration: an emerging axon death pathway linking injury and disease. Nat Rev Neurosci. 2014; 15:394–409. [PubMed: 24840802]
13. Raff MC, Whitmore AV, Finn JT. Axonal self-destruction and neurodegeneration. Science. 2002; 296:868–71. [PubMed: 11988563]
14. Wang JT, Medress ZA, Barres BA. Axon degeneration: molecular mechanisms of a self-destruction pathway. J Cell Biol. 2012; 196:7–18. [PubMed: 22232700]

15. Sasaki S, Maruyama S. Increase in diameter of the axonal initial segment is an early change in amyotrophic lateral sclerosis. J Neurol Sci. 1992; 110:114–120. [PubMed: 1506850]
16. Zhuo L, et al. hGFAP-cre transgenic mice for manipulation of glial and neuronal function in vivo. Genesis. 2001; 31:85–94. [PubMed: 11668683]
17. Clausen BE, et al. Conditional gene targeting in macrophages and granulocytes using LysMcre mice. Transgenic Res. 1999; 8:265–277. [PubMed: 10621974]
18. Lappe-Siefke C, et al. Disruption of Cnp1 uncouples oligodendroglial functions in axonal support and myelination. Nat Genet. 2003; 33:366–374. 2003. [PubMed: 12590258]
19. Parkhurst CN, et al. Microglia promote learning-dependent synapse formation through brain-derived neurotrophic factor. Cell. 2013; 155:1596–1609. [PubMed: 24360280]
20. Christofferson DE, Yuan J. Necroptosis as an alternative form of programmed cell death. Curr Opin Cell Biol. 2010; 22:263–268. [PubMed: 20045303]
21. Hitomi J, et al. Identification of a molecular signaling network that regulates a cellular necrotic cell death pathway. Cell. 2008; 135:1311–1323. [PubMed: 19109899]
22. Christofferson DE, et al. A novel role for RIP1 kinase in mediating TNFalpha production. Cell Death Dis. 2012; 3:e320. [PubMed: 22695613]
23. Polykratis A, et al. Cutting edge: RIPK1 Kinase inactive mice are viable and protected from TNF-induced necroptosis in vivo. J Immunol. 2014; 193:1539–1543. [PubMed: 25015821]
24. Ofengeim D, et al. Activation of Necroptosis in Multiple Sclerosis. Cell Rep. 2015; 10:1836–1849. [PubMed: 25801023]
25. Langfelder P, Horvath S. WGCNA: an R package for weighted correlation network analysis. BMC Bioinformatics. 2008; 9:559. [PubMed: 19114008]
26. Kigerl KA, et al. Identification of two distinct macrophage subsets with divergent effects causing either neurotoxicity or regeneration in the injured mouse spinal cord. J Neurosci. 2009; 29:13435–13444. [PubMed: 19864556]
27. Subramanian A, et al. Gene set enrichment analysis: a knowledge-based approach for interpreting genome-wide expression profiles. Proc Natl Acad Sci U S A. 2005; 102:15545–155550. [PubMed: 16199517]
28. Berger SI, Posner JM, Ma'ayan A. Genes2Networks: connecting lists of gene symbols using mammalian protein interactions databases. BMC Bioinformatics. 2007; 8:372. [PubMed: 17916244]
29. Kang SH, et al. Degeneration and impaired regeneration of gray matter oligodendrocytes in amyotrophic lateral sclerosis. Nat Neurosci. 2013; 16(5):571–9. [PubMed: 23542689]
30. Re DB, et al. Necroptosis drives motor neuron death in models of both sporadic and familial ALS. Neuron. 2014; 81:1001–1008. [PubMed: 24508385]
31. Gould TW, et al. Complete dissociation of motor neuron death from motor dysfunction by Bax deletion in a mouse model of ALS. J Neurosci. 2006; 26:8774–8786. [PubMed: 16928866]
32. Peschon JJ, et al. TNF receptor-deficient mice reveal divergent roles for p55 and p75 in several models of inflammation. J Immunol. 1998; 160:943–952. [PubMed: 9551933]
33. Osawa T, et al. Optineurin in neurodegenerative diseases. Neuropathology. 2011; 31:569–574. [PubMed: 21284751]
34. Deng HX, et al. Differential involvement of optineurin in amyotrophic lateral sclerosis with or without SOD1 mutations. Arch Neurol. 2011; 68:1057–1061. [PubMed: 21825243]
35. Newton K, Sun X, Dixit VM. Kinase RIP3 is dispensable for normal NF-kappa Bs, signaling by the B-cell and T-cell receptors, tumor necrosis factor receptor 1, and Toll-like receptors 2 and 4. Mol Cell Biol. 2004; 24:1464–1469. [PubMed: 14749364]
36. Chen Y, et al. Isolation and culture of rat and mouse oligodendrocyte precursor cells. Nature protocols. 2007; 2:1044–1051. [PubMed: 17546009]
37. Saura J, Tusell JM, Serratosa J. High-yield isolation of murine microglia by mild trypsinization. Glia. 2003; 44:183–189. [PubMed: 14603460]
38. Mayo L, et al. Regulation of astrocyte activation by glycolipids drives chronic CNS inflammation. Nat Med. 2014; 20:1147–1156. [PubMed: 25216636]

39. Wang H, et al. Mixed lineage kinase domain-like protein MLKL causes necrotic membrane disruption upon phosphorylation by RIP3. Mol Cell. 2014; 54:133–146. [PubMed: 24703947]

40. Xie X, et al. Systematic discovery of regulatory motifs in human promoters and 3′ UTRs by comparison of several mammals. Nature. 2005; 434:338–345. [PubMed: 15735639]

One Sentence Summary

RIPK1-mediated inflammatory and cell death mechanism may provide a common underlying etiology for mediating axonal pathology in ALS.

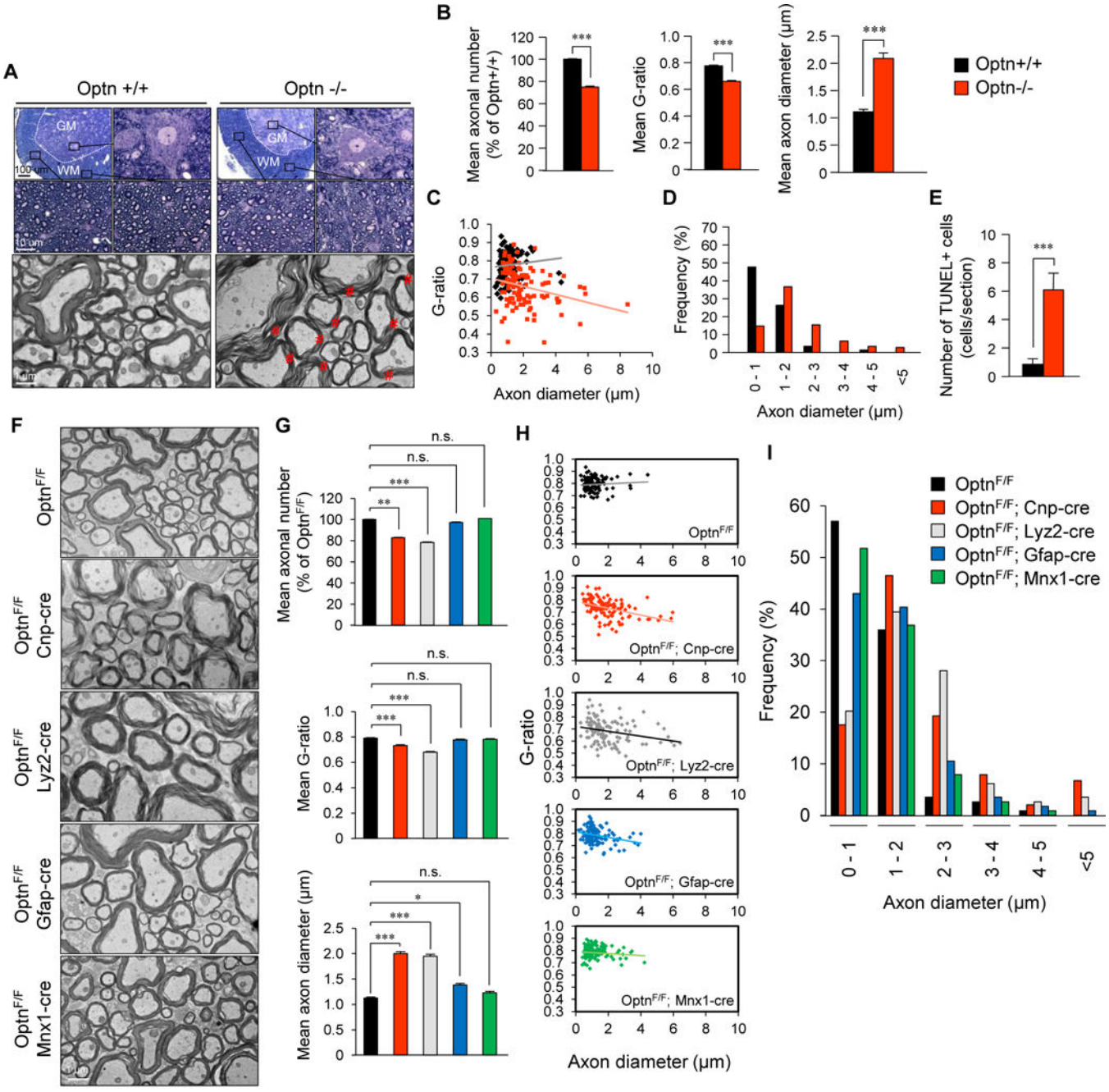

Fig. 1. Optn deficiency in oligodendrocyte and myeloid lineages promotes axonal loss and dysmyelination in the spinal cords of *Optn*−/− mice

(**A**) Top: Toluidine blue staining sections from the ventrolateral lumbar spinal cords of WT and *Optn*−/− mice. The brackets showing axons in the ventrolateral lumbar spinal cord white matter, and the motor neurons in the ventral lumbar spinal cord grey matter, respectively. Bottom, electron microscopic analysis of motor axonal myelination in the ventrolateral lumbar spinal cords from WT and *Optn*−/− mice. (**B–D; F–I**) The mean axonal numbers, mean g-ratios and mean axonal diameters, individual g-ratios distribution and distributions of axonal diameters in the ventrolateral lumbar spinal cord white matter (L1–L4) of WT,

Optn−/− mice, $Optn^{F/F}$ mice, $Optn^{F/F}$; *Cnp-cre* mice, $Optn^{F/F}$; *Lyz2-cre* mice, $Optn^{F/F}$; *Gfap-cre* mice and $Optn^{F/F}$; *Mnx1-cre* as indicated. (**E**) The number of TUNEL+ cells in the lumbar spinal cords (L1–L4, one section each) of indicated genotype (5 mice each genotype).

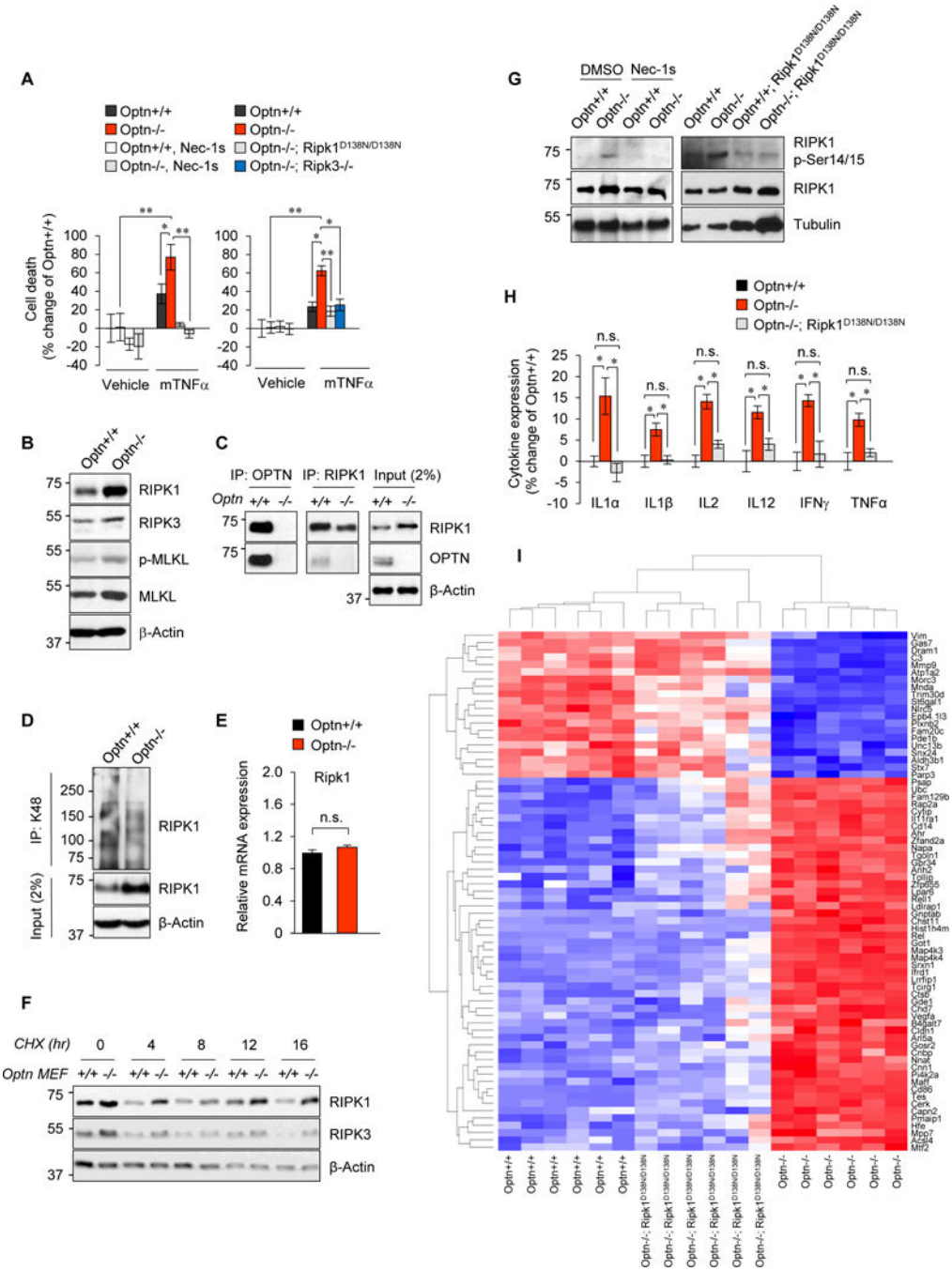

Fig. 2. OPTN deficiency sensitizes to necroptosis

(**A**) Murine primary oligodendrocytes of indicated genotypes were treated with mTNFα (10 ng/mL) +/or- Nec-1s (10 μM) for 24 hrs and cell death was assessed by using Toxilight assay (Lonza). Data are represented as the normalized means ± SEM, n=5–9 replicates per group. (**B**) The spinal cords of WT and *Optn*−/− mice were extracted with urea buffer and analyzed by western blotting using indicated abs. (**C**) The spinal cord lysates extracted with RIPA buffer were immunoprecipitated using anti-OPTN or anti-RIPK1 and the immunocomplexes were analyzed by western blotting using using indicated abs. (**D**) The

spinal cords from mice of indicated genotypes were lysed in 6M urea and immunoprecipitated using anti-K48 ubiquitin chain abs. The isolated immunocomplexes and input were analyzed by western blotting with anti-RIPK1. (**E**) The mRNA levels of RIPK1 in the spinal cords with indicated genotypes were measured by qRT-PCR. (**F**) WT and *Optn* −/− MEFs were treated with CHX (2 μg/ml) for indicated periods of time and the lysates were analyzed by western blotting using indicated antibodies. (**G**) Microglia from newborns of indicated genotypes were extracted in TX114 buffer and the western blots were probed with anti-RIPK1 p-S14/15 phosphorylation and anti-RIPK1. (**H**) The cytokine profiles in the spinal cords were measured using a cytokine array by ELISA. (**I**) Heatmap of top 71 genes in the module ME1 differentially expressed in microglia of indicated genotypes. Low expression is shown in blue and high expression in red.

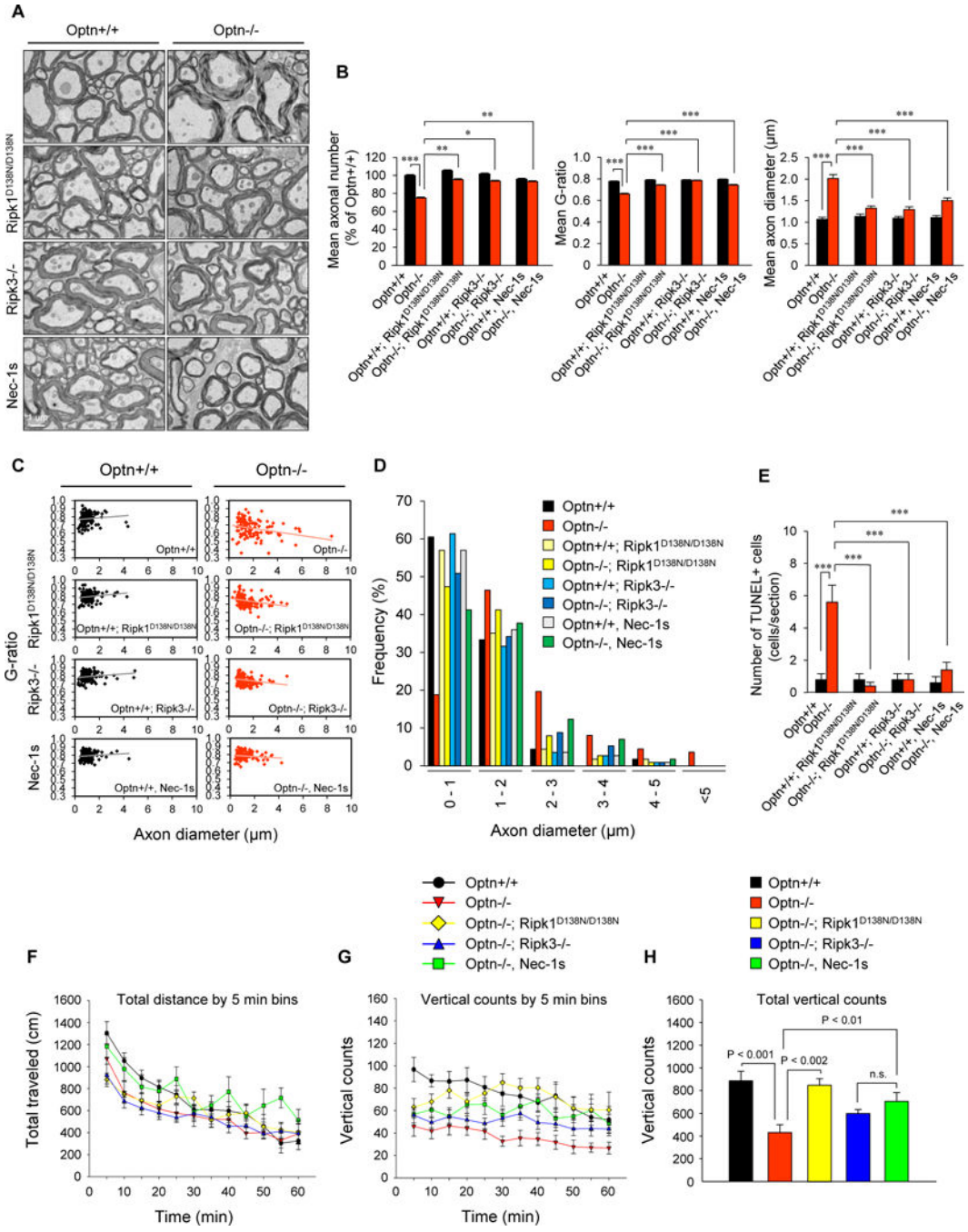

Fig. 3. RIPK1 and RIPK3 mediate axonal pathology in the spinal cords of *Optn*−/− mice

(**A**) Dysmyelination in the spinal cords of *Optn*−/− mice was blocked by genetically inhibiting RIPK1 in *Optn−/−; Ripk1*$^{D138N/D138N}$ mice, pharmacologically inhibiting RIPK1 by Nec-1s (oral dosing of Nec-1s for one month starting from 8 weeks of age) and by loss of RIPK3 in *Optn−/−; Ripk3*−/− mice. (**B–D**) Mean axonal numbers, g-ratios and axonal diameters (**B**), individual g-ratio distributions (**C**), and axonal diameter distributions (**D**). (**E**) The number of TUNEL+ cells in the lumbar spinal cords (L1–L4, one section each) of indicated genotypes at 3 months of age (5 mice per genotype). (**F–H**) Mice of indicated

genotypes were tested in Open Field Test for spontaneous motor activity. The mice were at 3 months of age and 28–32 g of body weight (no statistical significant difference on body weight between different groups). The total distance traveled in one hour showed no difference between different groups (**F**). *Optn*−/− mice showed a significant deficit on the vertical rearing activity (frequency with which the mice stood on their hind legs). This deficit was blocked after dosing with Nec-1s for one month starting from 8 weeks old and in *Optn*−/−; *Ripk1*$^{D138N/D138N}$ double mutant mice and reduced in *Optn*−/−; *Ripk3*−/− double mutant mice (**G–H**).

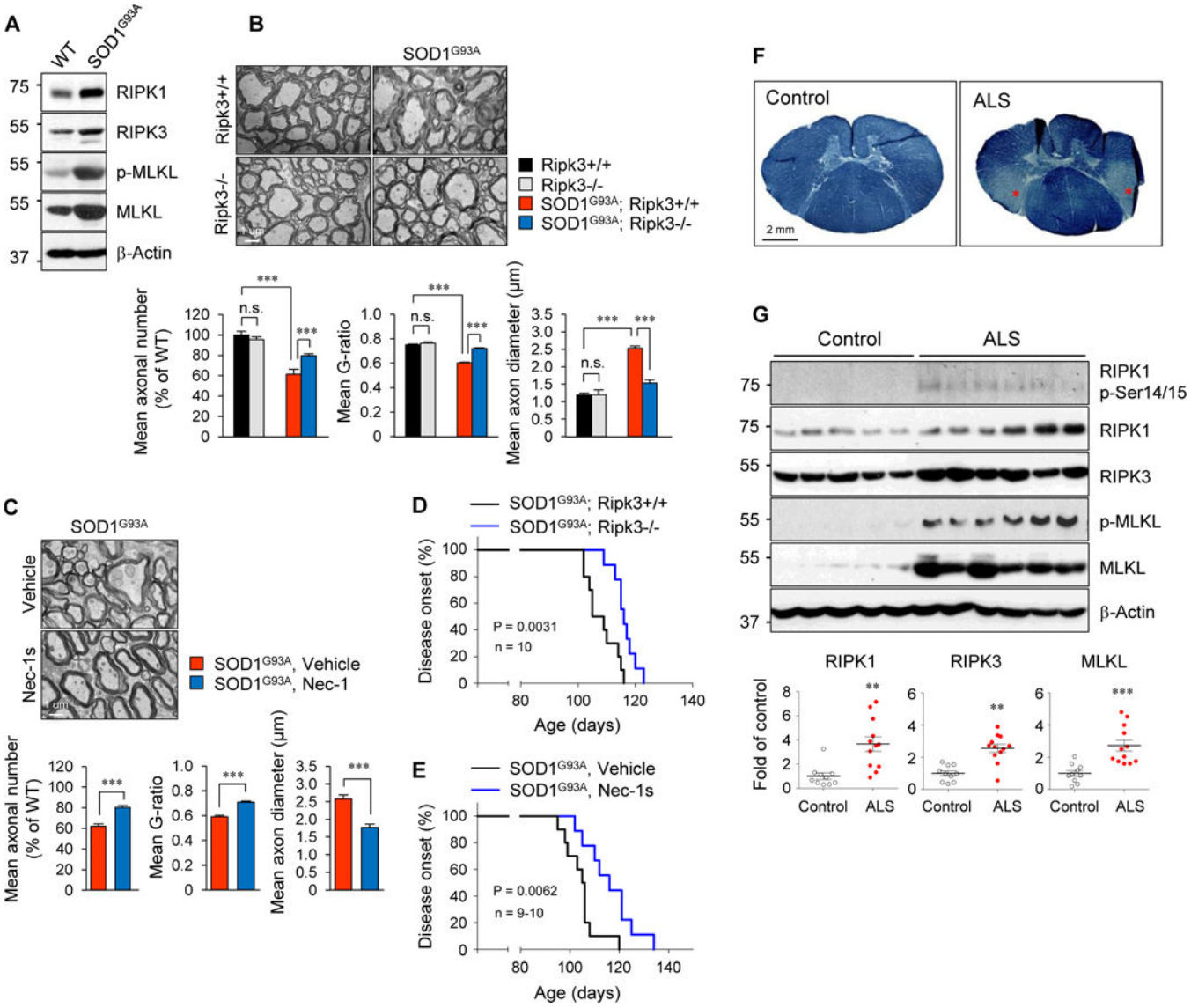

Fig. 4. RIPK1 and RIPK3 mediated axonal pathology is a common mechanism in ALS

(**A**) Urea buffer lysates of spinal cords from WT and *SOD1*^{G93A} transgenic mice (12 weeks of age) were analyzed by western blotting using indicated abs. (**B**–**C**) The myelination morphology (**top**), mean axonal numbers (**bottom**), mean g-ratios (**bottom**), mean axonal diameters (**bottom**) of the ventrolateral lumbar spinal cord white matter of *SOD1*^{G93A} mice, *SOD1*^{G93A}; *Ripk3*−/− mice (12 weeks of age) and *SOD1*^{G93A} mice dosed with vehicle or Nec-1s for one month starting from 8 weeks of age. (**D**–**E**) RIPK3 deficiency (**D**) and inhibition of RIPK1 by Nec-1s starting from 8 weeks of age (**E**) delayed the onset of motor dysfunction in SOD1^{G93A} mice. (**F**) Sections of pathological spinal cords from human control and an ALS patient were stained with luxol fast blue for myelin to show reduced myelination in the lateral column of lower spinal cords of ALS. (**G**) Western blotting analysis of human control and ALS spinal cord samples using indicated abs (**top**) and the

quantitation of RIPK1, RIPK3 and MLKL levels from 10 controls and 13 ALS cases (**bottom**).